Article published online: 2021-08-02

Bone marrow lesions: A systematic diagnostic approach

Filippo Del Grande, Sahar J Farahani, John A Carrino, Avneesh Chhabra

The Russell H. Morgan Departments of Radiology and Radiology Science, Johns Hopkins Hospital, Baltimore, MD 21287, USA

Correspondence: Dr. Avneesh Chhabra, The Russell H. Morgan Departments of Radiology and Radiological Science, The Johns Hopkins Medical Institutions, 601 North Wolfe Street, Baltimore, MD 21287, USA. E-mail: achhabr6@jhmi.edu

Abstract

Bone marrow lesions on magnetic resonance (MR) imaging are common and may be seen with various pathologies. The authors outline a systematic diagnostic approach with proposed categorization of various etiologies of bone marrow lesions. Utilization of typical imaging features on conventional MR imaging techniques and other problem-solving techniques, such as chemical shift imaging and diffusion-weighted imaging (DWI), to achieve accurate final diagnosis has been highlighted.

Key words: Bone marrow lesion; chemical shift imaging; diffusion; magnetic resonance imaging

Introduction

Bone marrow lesions are a common and non-specific magnetic resonance imaging finding associated with various pathologies. Unless a systematic approach is followed, it may cause confusion in the differential diagnosis. Based on the type and relative proportion of signal alterations on conventional T1-weighted (TIW) and T2-weighted (T2W) MR images, various etiologies of bone marrow lesions can be divided into three categories [Table 1]. This article outlines a systematic approach using this categorization, typical imaging features of various pathologies based on available literature, and prudent use of problem-solving imaging techniques, such as chemical shift imaging (CSI) and diffusion-weighted imaging (DWI). We believe that this approach could help the radiologist to better diagnose the etiology of bone marrow lesions, confirm the clinical diagnosis, and aid in appropriate patient management.

Access this article online	
Quick Response Code:	Website: www.ijri.org
	DOI: 10.4103/0971-3026.137049

Normal Bone Marrow

The normal bone marrow is constituted in different proportions by red (hematopoietic bone marrow) and yellow marrow (hematopoietic inactive marrow), which have different MRI characteristics due to the different content of hematopoietic and fat cells. Red marrow contains 40% fat cells, 40% water, and 20% hematopoietic cells, whereas yellow bone marrow is composed of 80% fat cells, 15% water, and 5% hematopoietic cells.[1] After infancy, red marrow to yellow marrow conversion progresses from the periphery (appendicular skeleton) to the center (axial skeleton) and from the diaphysis to the metaphysis in long bones.[1] Epiphysis and apophysis are the first to convert to yellow marrow, which usually happens in the first decade of life itself. In long bones, such as humerus and femur, crescentic subchondral area of residual red marrow is commonly present. In an adult, the red marrow is mainly located in the appendicular skeleton in the metaphysis and near the vertebral endplate (the methaphyseal equivalent), due to well-developed vascularity.[2,3]

Imaging Technique

The initial evaluation may include radiography; however, many bone marrow lesions are occult on conventional radiography and MR imaging might be the first modality on which they show up for the first time. Attention to appropriate MR imaging technique is important. The

Table 1: Etiologies of bone marrow lesions-proposed categorization

Category I	Category II	Category III
Traumatic	Neoplastic	Metabolic/hematopoietic disorders
Insufficiency/stress fractures	Infection	Neuropathic disorders
Complex regional pain syndrome		Chemotherapy- and radiotherapy-related marrow changes
Inflammatory arthropathy		Paget's disease
Degenerative osteoarthritis		Antiretroviral therapy in HIV patients/serous marrow lesions
Active bone infarct/ischemia		

HIV: Human immunodeficiency virus

imaging can be performed on 1.5 T or 3 T MR scanners. The conventional techniques include T1W (keep echo time, TE <8 ms on 1.5 T and <10 ms on 3 T) and T2W, fat-suppressed T2W, or short tau inversion recovery (STIR; for STIR, keep TE ~25-35 ms to maintain good signal to noise ratio) pulse sequences. Post-contrast (intravenous gadolinium) fat-suppressed T1W imaging should always include pre-contrast baseline fat-suppressed T1W imaging in at least one plane, with subtraction manipulation if possible. Problem-solving techniques are performed in a suspected or known marrow lesion in a short period of time. These include DWI (diffusion moments, single-shot spin-echo echo-planar imaging, *b* values 50, 400, 800 s/mm^2, axial plane acquisition, frequency selective fat suppression), CSI (in- and out-of-phase imaging, CSI or two-point Dixon technique using gradient echo imaging), and single-voxel or multivoxel spectroscopy (MRS). Two-point Dixon technique (~5 min) takes longer than CSI (2-3 min); however, one can obtain a number of images from the same acquisition, "water only," "fat only," and "both water and fat" images. Good shimming is essential before DWI or MRS to obtain the best imaging possible. To avoid ghosting artifacts from eddy current distortions and poor fat suppression, tighter echo spacing, avoiding motion and frequency selective fat suppression are useful on diffusion imaging.

On conventional radiography, the normal marrow and red marrow reconversion areas do not exhibit any alterations in density, reflecting poor sensitivity of radiography in marrow lesions. As a general rule, the normal marrow (red or yellow marrow) in adult is hyperintense on T1W MR image as compared to the adjacent muscle or, in the spine, as compared to the intervertebral disc/paraspinal muscle.[4] Moreover, the red marrow shows signal intensity less than that of fat on T2W MR images. STIR or fat-suppressed T2W MR (fsT2-W) imaging techniques are most sensitive for the detection of bone marrow lesions due to increased dynamic range of contrast. With increasing use of proton density sequence instead of T1W sequence in routine joint imaging, it should be noted that the normal or reconverted red marrow may appear isointense to the muscle. Additionally, sometimes, the residual/reconverted red marrow may show patchy distribution mimicking lesions. In those cases, simple looking back at the planning scout images (generally performed as gradient echo images) may be helpful. The focal islands of normal marrow always have some amount of microscopic fat and, therefore, tend to lose signal on these images (technically out-of-phase). However, if the scout image is performed as an in-phase image or if the lesion is not covered on the scout image, additional CSI would confirm that the lesion does not replace the bone marrow by demonstrating 20% signal loss on the out-of-phase images. It is important to emphasize that CSI does not differentiate between benign and malignant lesions but between bone marrow replacing and non bone marrow replacing lesions. In fact, a benign bone marrow replacing lesion, such a bone cyst would show a drop of signal in out-of-phase images less than 20% compared to in-phase images. Yellow marrow follows the same signal intensity as the subcutaneous fat. The enhancement of the normal marrow in adults is usually less than 35% from baseline on intravenous gadolinium administration.[5] According to Disler and colleagues, a relative signal intensity ratio of 0.81 using CSI has a sensitivity and specificity of 95% to detect bone marrow neoplasm.[6] Zampa and co-workers found sensitivity, specificity, accuracy, positive predictive value, and negative predictive value of 88.8, 80.5, 84.9, 83.3, and 86.4%, respectively, using opposed phase gradient techniques and a signal intensity ratio cut-off of 1.2 to differentiate between benign and malignant vertebral lesions.[7] It is important to remember that a normal marrow appearance on MR imaging does not definitely exclude marrow infiltration. Since the MR imaging appearance of the bone marrow depends on the proportion of fat cells and hematopoietic cells, in cases of early/minimal infiltrations that do not significantly change this equilibrium, the MR signal may not be altered.[5] On DWI, diffusion restriction is noted in focal or diffuse marrow lesions due to increased cellularity with cell membrane restrictions with these lesions. It has proven to be a useful method in identification of marrow pathology. Lower apparent diffusion coefficient (ADC) lower than 1.1-1.2x10-3 mm/s2 values are usually seen with high cellularity or malignancy.[8] Baur and colleagues studied 39 vertebral compression fractures and concluded that DWI is a good technique to differentiate between benign and malignant fractures. Benign compression fractures were iso- to hypointense to normal vertebral body, whereas malignant fractures were hyperintense.[9]

Categorization of Bone Marrow Lesions

Based on the type and relative proportion of signal alterations on conventional T1W and T2W MRI images, various etiologies of bone marrow lesions can conveniently be divided into three categories [Table 1]. Category I includes bone marrow lesions related to trauma, insufficiency injury, aseptic necrosis, biomechanical, disuse,complex regional pain syndrome (CRPS), transient osteoporosis of hip, or

degenerative/inflammatory etiologies. Category II includes aggressive processes, such as infections or neoplastic conditions. Category III includes pathologies with complex/mixed phenomena, such as metabolic, hematopoietic, treated infiltrative malignancies, HIV treatment associated lipodystrophy, serous marrow lesions, and Paget's disease. Further discussion will be focused on general MR imaging features of these categories on conventional sequences, typical MR imaging features of various entities within these categories, and the role of problem-solving techniques aiding in their definitive diagnosis [Tables 2 and 3].

Category I Lesions

In this category, the high signal intensity alteration on fluid-sensitive sequences (STIR/fsT2-W/fat-saturated proton density-weighted (fs PD-W)) is much more pronounced than the low signal intensity on T1W sequence. The etiologies are usually benign and, in some part, encompass a component of stress reaction/hyperemia. The lesions show homogenous bone marrow edema and usually they do not have associated soft tissue component or solid enhancement. Focal lesions are generally absent, unless there is associated intraosseus hematoma related to a recent fracture, focal half-moon-shaped or serpiginous lesion of aseptic necrosis, or subchondral degenerative/subcortical avulsive cystic changes. Problem-solving techniques, such as CSI and DWI, are rarely needed for diagnosis. Conventional radiography is usually negative in marrow-centric stress or microtrabecular injuries. However, more significant or larger lesions may show up as fractures, avascular necrosis (AVN), or osteopenia from disuse/CRPS.

Probably, the most common pattern in this category is acute or chronic traumatic injury, which may range from bone contusion, sometimes referred as "bone bruises," to a real fracture. Histologically, the traumatic bone marrow lesion is the result of hemorrhage and inter-trabecular microfractures.[10] MR imaging plays an important role in the assessment of stress injuries/fractures [Figure 1A-D] due to the relative low sensitivity of radiographs, ranging from 15-35% on initial examination to 30-70% on follow-up examination.[11] Stress fractures are of two types, fatigue and insufficiency. Fatigue fractures are the result of abnormal stress on normal bone structure, whereas insufficiency fractures are the result of a normal stress on an abnormal bone, such as in osteoporosis and osteomalacia. The former are more common in young athletes and military recruits and the latter in older patients.[11,12] Stress injuries were classified by Fredericson *et al*. into four grades based on the conventional MR imaging characteristics. Grade I injury represents periosteal edema, Grade II represents mild bone marrow edema visible only on fsT2-W sequence but not on T1W sequence, Grade III (inter-trabecular

Table 2: Normal and abnormal bone marrow

MR technique	MR sequence	Normal marrow or RMR	Pathologic marrow
Conventional	T1-W SE	SI>muscle/disc	SI=or<muscle/disc
	PD-W/T2-W	Minimally increased SI<fat	SI approaching or similar to fat
	STIR/fsT2-W/fsPD-W	Minimally increased SI. Less commonly, focal islands of red marrow	Increased SI approaching vessels/epi-apophysis involvement/focal lesions/soft tissue mass
	T1-W-IV Gad	<35 % Enhancement	>35 % Enhancement
Problem solving techniques	CSI	>20 % SI loss on out-of-phase imaging	<20 % SI loss/increased SI on out-of-phase imaging
	DWI	No diffusion restriction	Diffusion restriction
	MRS	No Choline peak	Choline peak

SI: Signal intensity, Gad: Gadolinium, CSI: Chemical shift imaging, DWI: Diffusion-weighted imaging, MRS: MR spectroscopy, STIR: Short tau inversion recovery, PD-W: Proton density weighted, GRE: Gradient echo, RMR: Red marrow reconversion

Table 3: MRI characteristics of various categories of bone marrow lesions

MR technique	MR sequences	Category I	Category II	Category III
Conventional	T1-W SE	SI>muscle/disc	SI<<muscle/disc	Heterogeneous SI=, > or <muscle/disc
	PD-W/T2-W TSE	SI approaching or similar to fat	SI approaching or similar to fat	Heterogeneous increased or decreased SI
	STIR/fsT2-W/fsPD-W	Increased signal approaching vessels/epi-apophysis, generally no focal lesions	Increased signal approaching vessels/epi-apophysis involvement, focal lesions	Heterogeneous increased or decreased SI with or without focal lesions
	T1-W-IV Gad	Minimal enhancement	Intense enhancement	Minimal to none enhancement
Problem-solving techniques	CSI	>20 % SI loss on out-of-phase imaging	Neoplasm: <20 % SI loss/no SI loss/increased SI on out-of-phase imaging Infection: SI loss on out-of-phase imaging ±	>20 % SI loss on out-of-phase imaging
	DWI	Usually no diffusion restriction	Neoplasm/pus: Diffusion restriction	Usually no diffusion restriction
	MRS	No choline peak	Neoplasm; choline peak	No choline peak

SI: Signal intensity, Gad: Gadolinium, CSI: Chemical shift imaging, DWI: Diffusion-weighted imaging, MRS: MR spectroscopy, STIR: Short tau inversion recovery, PD-W: Proton density weighted, GRE: Gradient echo, RMR: Red marrow reconversion, TSE: Turbo spin echo

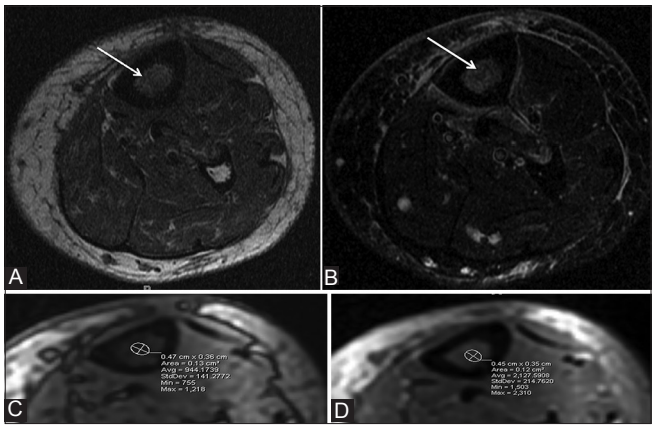

Figure 1 (A–D): Axial T1W (A) and STIR (B) images at the level of the mid-tibia. There is homogenous ill-defined bone marrow lesion, appearing mildly hyperintense to muscle on T1W and moderately hyperintense on STIR images (arrows). Associated fascial and periosteal edema is also present. Chemical shift imaging (CSI) shows more than 20% loss of signal intensity (SI) on the out-of-phase image (C) compared to the in-phase image (D). Bone marrow lesions category I (stress reaction)

fracture) represents extensive edema visible on all sequences (however, it is much more pronounced on fluid-sensitive sequence), and Grade IV represents a clear fracture line (which may be incomplete/complete and may be displaced/non-displaced).[13] Grade I/II injuries reflect stress response/reaction and Grade III/IV injuries represent fractures. The fracture line is commonly visible as a linear, solid or broken T1 and T2 hypointensity surrounded by a cloud of edema. Several reports on stress fracture in athletes are available and virtually every bone can be involved depending on the type of activity. Typical location for stress fractures are the pelvis with lesser trochanter, femoral neck, tibia, and sacrum from running; and shoulder in athletes involved in throwing and lifting, such as in baseball players.[14-16] Rarer locations are: rib fractures in weightlifters, olecranon in baseball players, hook of the hamate in golf players, tennis players, or baseball players, and proximal ulna in throwing athletes.[17-20]

Insufficiency fractures affect mainly elderly patients with osteoporosis. A survey of 60 cases showed that the mean age of the patients was 72.5 years for women and 59.5 years for men.[21] Osteoporotic vertebral fractures and insufficiency fractures of the sacrum are a well-known cause of low back pain in elderly women.[22] Insufficiency fracture of the knee, previously known as spontaneous osteonecrosis of the knee (SONK), was thought to be the result of osteonecrosis, but more recent data suggests that these injuries, in most cases, represent subchondral insufficiency fracture of the medial femur condyle or medial tibial plateau in the setting of meniscal tears/recent meniscectomy.[23] These fractures are commonly seen as a subtle focal subchondral area of T2 hypointensity in the background of extensive bone marrow edema and fascial edema in the acute stages and subsequently convert into subchondral sclerosis/cystic change in subacute/chronic stages. Most subjects with subchondral insufficiency injuries experience sudden pain and do not, in general, have any systematic disease, whereas patients with osteonecrosis present with insidious onset of pain and have underlying systemic disease. Moreover, the imaging features of osteonecrosis (AVN) are different. AVN is commonly seen as a half-moon-shaped lesion or a serpiginous lesion with a "double line" sign on T2W images, which is characterized by a peripheral low-intensity rim and inner high-intensity line. Additionally, the marrow inside the lesion may be isointense to the normal bone marrow or may sometimes contain fat/edema or hemorrhage.[24] Finally, osteonecrosis shows relatively mild bone marrow lesions and fascial edema, as compared to insufficiency fractures.[25]

CRPS is another condition associated with bone marrow edema. The pattern in these patients is mainly localized in the foot, tibia, and femur in descending order. The appearance is patchy/reticular and more diffuse compared to the bone marrow edema in stress reaction.[26] Depending upon the stage of disease, soft tissue edema(acute/subacute stage) and soft tissue atrophy (chronic stage) may be associated.[26, 27] However, two important pitfalls should be kept in mind. In children and adolescents, patchy/reticular appearance of the marrow may be normally observed with patchy red marrow conversion. In those cases, an asymmetric larger confluent area of more T2 brightness should be looked for the diagnosis of pathologies such as superimposed bone contusion or fracture or infection. Also, disuse osteoporosis can give similar marrow appearance, e.g. foot and ankle of a person with previous cast placement in the proximal leg or knee may show marrow signal abnormality identical to the CRPS. Therefore, the findings should be clinically correlated for appropriate diagnosis.

Bone marrow edema is very common in osteoarthritis (OA) as well as in both seropositive and seronegative inflammatory arthropathies. While OA results in asymmetric findings (unicompartment/single joint), inflammatory arthropathies frequently involve multiple joints, or may produce relatively symmetric disease. Several studies have demonstrated that in OA patients, bone marrow edema is related to damage of overlying cartilages, with subchondral edema-like changes that progress into cysts over time.[28-31] Zaho *et al*. in their study found a correlation between bone marrow edema and more advanced cartilage lesions at 12 months follow-up of 19 patients with knee OA.[28] A 30-month follow-up of 1344 OA patients with knee MRI revealed that meniscus pathology correlates with occurrence as well as worsening of bone marrow edema.[29] These findings were confirmed by another study that found a correlation between bone marrow edema and ipsilateral medial and lateral meniscus lesions.[30] According to Crema *et al*. who studied 1283 knee MRI exams, subchondral cyst-like lesions develop in the region of bone marrow edema in individuals who have or are at risk to have OA.[31] Zanetti *et al*. studied the histological

findings of the bone marrow edema of 16 patients referred for total knee replacement due to OA.[32] The conclusion of the authors was interesting, in the sense that the bone marrow edema pattern on MRI was mainly the result of bone marrow necrosis, bone marrow fibrosis, and trabecular abnormalities while edema was only a minor component.

Transient osteoporosis of hip is a much less common condition than previously thought/reported. Most of these patients have an underlying subchondral insufficiency fracture or stress response. Histologically, it may correlate with edematous changes, mild fibrosis, vascular congestion, and/or interstitial edema without osteonecrosis in femoral head.[33] On MR imaging, the lesion homogenously involves the femoral head and, sometimes, may extend to the femoral neck.[34-36] There may also be associated minimal joint effusion and fascial edema. Similar to other category I lesions, the bone marrow edema is more pronounced on T2W imaging than on T1W imaging.[36] According to Vande Berg *et al*., lack of subchondral changes in T2W sequence and/or on post-contrast T1W sequence has 100% positive predictive value for the diagnosis of transient osteoporosis.[37]

Category II Lesions

This category includes important pathologies which usually show aggressive behavior and poorer prognosis, if not treated appropriately. The two major entities include infection and tumor. Conventional radiography plays an important role in the identification and characterization of these lesions, especially the presence of benign or malignant periostitis, focal lytic or sclerotic lesions, and cortical destruction or permeation. These pathologies are generally associated with soft tissue masses and/or fluid collections and have more pronounced lower signal intensity than muscles on T1W sequence, compared to the lesions in category I. Focal lesions are commonly seen with neoplastic etiology. Multiple/multifocal lesions may be observed with primary malignancies associated with skip lesions, or with bony metastases/lymphoma. In infectious cases, Brodie's abscess may be seen as a confluent oval or elongated lesion approaching the physeal plate. Two layers of the abscess wall may be apparent similar to layers of granulation tissue (outer)/mineralized (inner) layer, as observed with organized abscesses in other solid soft tissue viscera, such as liver. Additionally, extensive soft tissue edema in the adjacent fascial planes/fat pads and fluid collections are important markers of infection as opposed to malignancy.

Diffusely infiltrative malignancy, such as leukemia [Figure 2A-E], lymphoma, and breast metastases [Figure 3A-F], could be sometimes difficult to differentiate from diffuse red marrow reconversion. Problem-solving techniques, such as CSI [Figures 2C, D and 3E, F] and DWI [Figure 3G], are prudently used for diagnosis to differentiate tumors from focal islands of normal marrow or other benign bone marrow lesions. The use of in-phase and out-of-phase imaging is probably the best known problem-solving technique for bone marrow pathologies. Disler *et al*. found that in-phase and out-of-phase imaging was helpful to predict the malignancy in a bone lesion.[6] Several other articles confirmed the data and substantiated the utility of CSI to distinguish benign from malignant vertebral lesions.[7,38,39] Recently, Zajick *et al.* proposed a cut-off decrease of more than 20% of the signal intensity in out-of-phase imaging to predict malignancy in vertebral body abnormality.[40] DWI is another technique which may help differentiate malignant from benign lesions. Several research articles have documented that restrictive diffusion with high signal intensity on DWI is observed in neoplastic (pathologic) fractures as compared to osteoporotic fractures.[9,41-43] To our knowledge, Bauer *et al*. were the first authors to address the utility of DWI to differentiate benign from malignant spine lesions.[9] The authors analyzed 39 compression fractures with DWI. According to their study, malignant vertebral fractures showed high signal intensity on DWI, whereas benign lesions showed low signal intensity. On the contrary, literature on osteomyelitis and tumors of the peripheral skeleton is very scant compared to that on spine. Yasumoto *et al*. found that DWI had a high specificity to detect bone marrow infiltration with

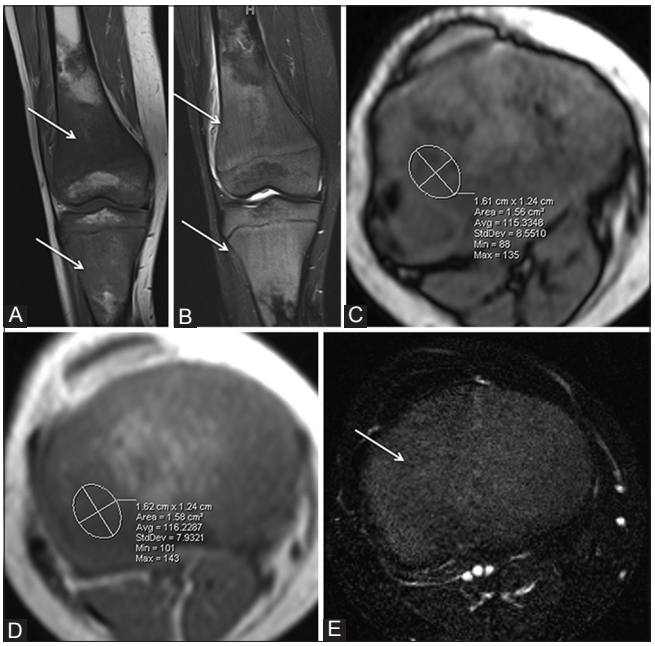

Figure 2 (A-E): Coronal T1W (A) and STIR (B) images through the knee show diffuse bone marrow lesions, homogeneously hypo-isointense on T1W and moderately hyperintense on STIR images, involving distal femur and proximal tibia with epiphyseal involvement (arrows). CSI confirms the marrow replacement due to lack of drop in signal intensity on the out-of-phase image (C) compared to in-phase image (D). Post intravenous gadolinium axial T1W subtraction imaging (E) at the level of the proximal tibia shows diffuse enhancement (large arrow) similar to adjacent vessels (small arrow). Bone marrow lesions category II

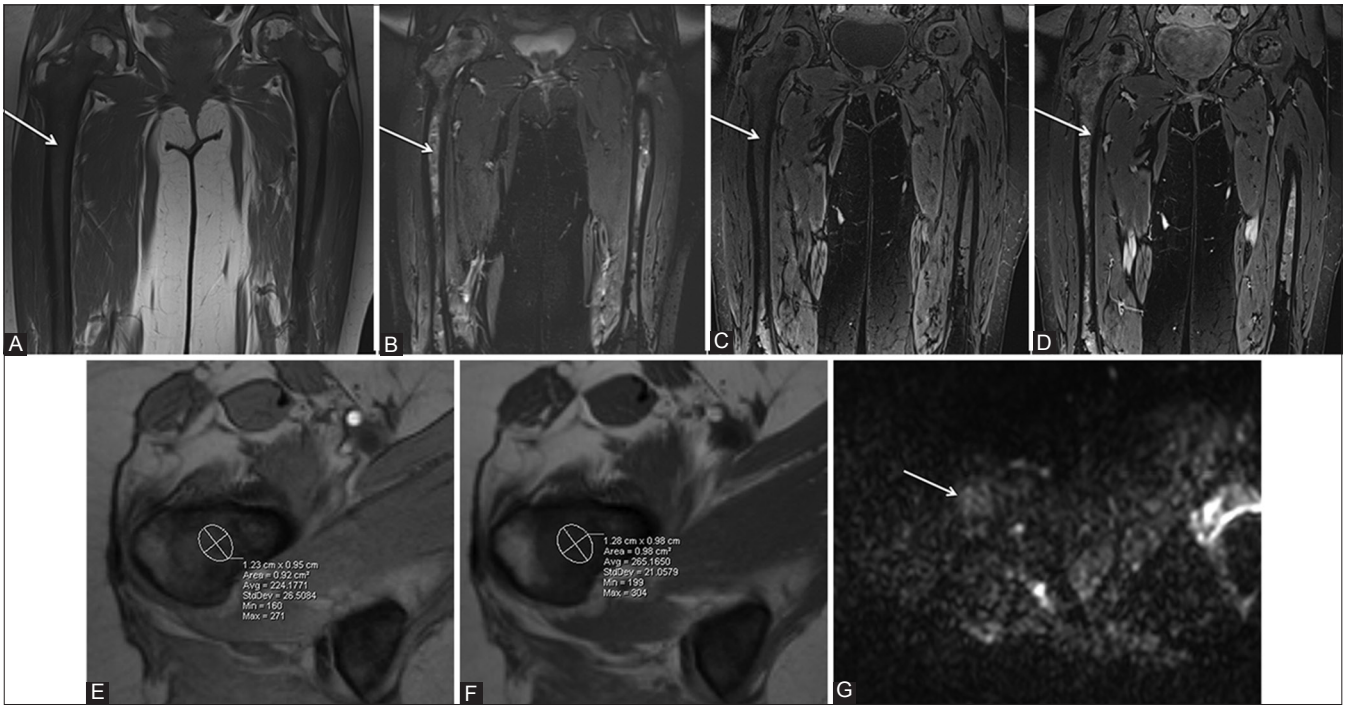

Figure 3 (A-G): Coronal T1W (A) and coronal 3D STIR (B) images through both thighs. There are diffuse and inhomogeneous bone marrow lesions with hypointense signal intensity of the femurs on T1W and moderately hyperintense on STIR images with bilateral epiphyseal involvement. Corresponding coronal pre- (C) and post-gadolinium (D) 3D T1W images show diffuse enhancement of the lesions. The drop of signal intensity SI on out-of-phase image (E) is less than 20% (F). DWI (G) image at the level of the proximal right femoral shaft shows restricted diffusion (arrow). Bone marrow lesions category II

malignant lymphoma.[44] Herneth *et al*. reported several cases of peripheral osteomyelitis with increased tissue diffusivity.[45] These findings were confirmed by some other studies on skull base osteomyelitis that did not show diffusion restriction either.[46, 47] Therefore, it seems plausible that ADC lower than 1.1-1.2x10-3 mm/s2 values can aid in distinguishing osteomyelitis from neoplasm. On the contrary, Pui *et al*. reported 69 tuberculous, 9 pyogenic, and 50 malignant marrow lesions that showed similarly restricted ADC values.[48] However, more studies are needed to explore the role of fractionated ADC values rather than mean ADC values using multiple *b* values (diffusion moments) to assess the utility of this novel technique.[49] MRS is an experimental technique, although Choline peak seems to be a reliable indicator of increased cellularity.[50] To the best of our knowledge, there is no data exploring MRS in osteomyelitis, except for an isolated case among 36 patients reported by Wang *et al*.[50] In this series, the patient with tuberculosis arthritis did not show a Choline peak. MRS has been reported to be useful in bone marrow lipid assessment in osteoporosis.[51]

Having discussed both conventional and advanced MR techniques, one of the most important MRI indications in this category is the assessment of osteomyelitis in the adult population with diabetic foot. Diabetic pedal osteomyelitis is almost always the result of spread of infection from a skin ulcer and occurs most frequently around the fifth and first metatarso-phalangeal joints and calcaneocuboid joint.[52] Confluent areas of low signal intensity on T1W sequence are an important feature used to differentiate osteomyelitis from reactive bone marrow edema. Reactive edema shows bone marrow edema similar to category I lesions, with predominantly high signal intensity on fluid-sensitive sequence and either a normal bone marrow or a hazy subcortical reticular distribution of hypointensity on T1W sequence.[53] One should not overlook cortical destruction (loss of expected T1 hypointensity of the cortex) as an important sign of osteomyelitis on MR imaging, similar to the one used on radiographs. This sign is particularly well seen on gadolinium-enhanced images, similar to fluid collections/sinus tract associated with infections. One challenging differential diagnosis for the radiologist is to distinguish osteomyelitis from neuropathic joint. In the acute stage, the imaging findings of the neuropathic joint are very similar to those of osteomyelitis, with features such as subchondral T1 low signal intensity, T2 high signal intensity, and joint effusion.[54, 55] In the subacute and chronic stages, there is progressive bone erosion, subchondral cyst formation, bone destruction, debris, disorganization, dislocation, and decreasing bone marrow edema. The most reliable criteria that favor neuropathic arthropathy over osteomyelitis are predisposition for tarso-metatarsal joints, bilateralism, and the lack of soft tissue findings of infection such as skin ulcer, abscess, and/or sinus tract.[56] Moreover, the disappearance of previously present subchondral cysts

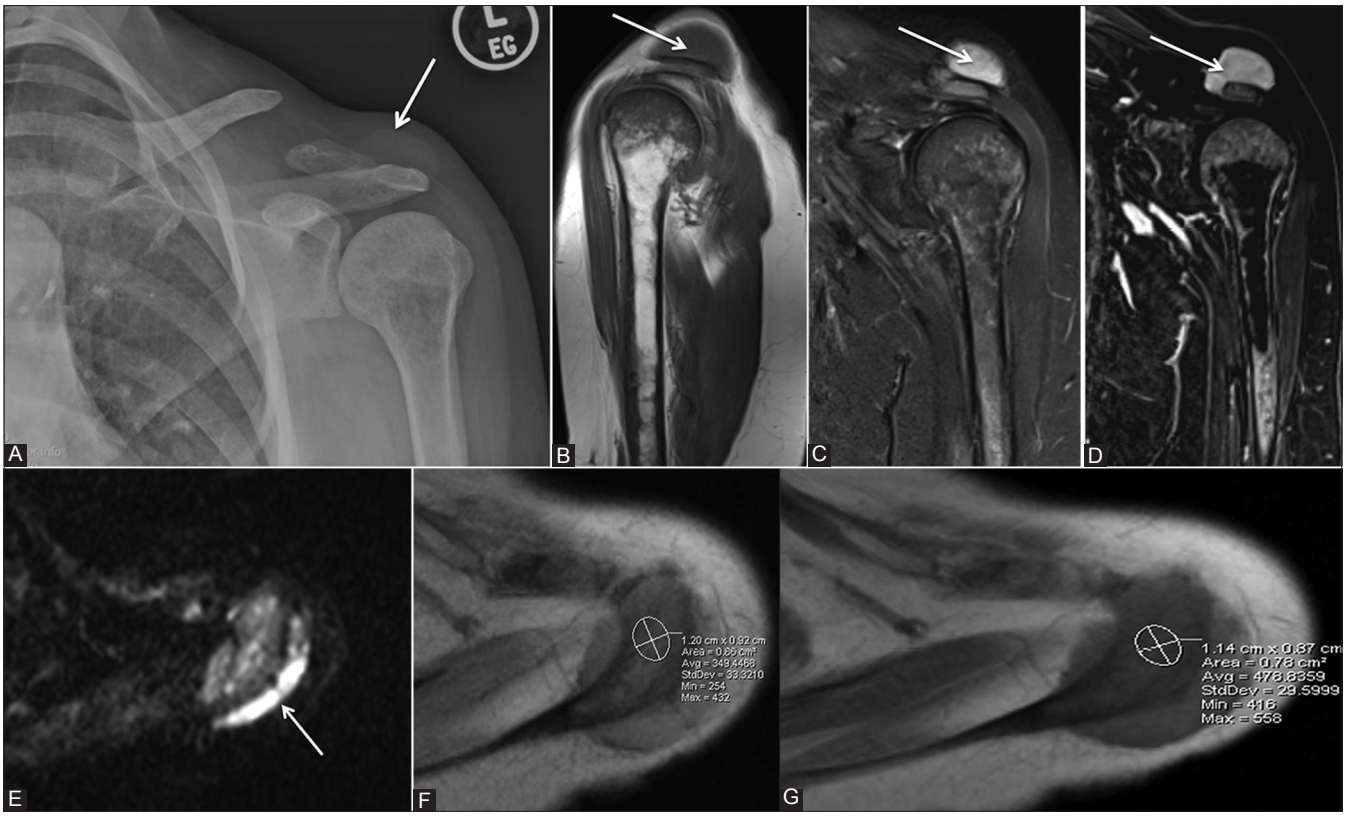

Figure 4 (A-G): Frontal radiograph shows patchy marrow sclerosis and mass (arrow). Sagittal T1W (B) and coronal STIR (C) images show patchy marrow replacement with epiphyseal involvement of the proximal humerus. Associated subcutaneous soft tissue mass shows marked T2 hyperintensity and intense enhancement (arrows) on post-contrast subtracted 3D T1W image (D). Restricted diffusion was seen in the acromion and soft tissue mass, reflecting high cellularity (arrow in E), and there was >20% signal loss on the out-of-phase (F,G) image. Bone marrow lesions category III

favors osteomyelitis. Additionally, "ghost sign," referring to a low signal intensity bone structure on T1W sequence that "reappears" as high signal intensity on fluid-sensitive sequence, suggests superimposed osteomyelitis.[56]

Category III lesions

Category III lesions show complex and more heterogeneous alterations of density on conventional radiography and signal intensity on T1W and T2W MR images. There may be associated focal lesions, but usually there are no associated soft tissue masses and/or fluid collections, except areas of extramedullary hematopoesis, which can be seen in hematopoetic disorders [Figure 4A-G]. This category encompasses pathologies such as, metabolic/hematopoietic disorders including Gaucher's disease, thalassemia, and sickle cell disease, in which marrow MR signal alterations are frequently complicated by aseptic necrosis/infections/blood transfusion related blood product deposition. Other conditions include infiltrative malignancy treated by chemo-radiation/bone marrow transplant, Paget's disease in acute-subacute phases, and serous marrow lesions observed in HIV-infected patients having lipodystrophy syndrome treated with highly active antiretroviral therapy.[57-59] These conditions can be highly heterogeneous and difficult to distinguish from active malignancy. However, there are usually small islands of microscopic fatty marrow in successfully treated lesions.[58] Therefore, imaging findings should be correlated with clinical findings and other available biochemical results, and problem-solving techniques such as CSI [Figure 4F-G] and DWI [Figure 4E] should be frequently employed in these cases for exclusion of malignancy. Additionally, DWI may also be used to assess treatment response in tumors, as increasing ADC values (reflecting necrosis/apoptosis) usually correlate with good treatment response.[60] Finally, a unique pattern of diffusely hypointense marrow on all MR imaging sequences may be observed in a limited number of conditions such as hemosiderosis, sclerotic bone conditions such as renal osteodystrophy/osteopetrosis/pyknodysostosis/fluorosis, and myelofibrosis. MR imaging is helpful in finding superimposed complications such as infection/stress reaction/fracture by demonstrating T2-hyperintense edema and/or enhancement at the respective site (s) of insult.

To conclude, bone marrow lesion can be seen as a non-specific finding in a variety of conditions. A systematic approach to its evaluation by categorization is essential with prudent use of both conventional and problem-solving techniques, such as CSI and DWI, for accurate diagnosis and appropriate patient management.

References

1. Vogler JB 3rd, Murphy WA. Bone marrow imaging. Radiology 1988;168:679-93.
2. De Bruyn PP, Breen PC, Thomas TB. The microcirculation of the bone marrow. Anat Rec 1970;168:55-68.
3. Weiss L. The structure of bone marrow. Functional interrelationships of vascular and hematopoietic compartments in experimental hemolytic anemia: An electron microscopic study. J Morphol 1965;117:467-537.
4. Carroll KW, Feller JF, Tirman PF. Useful internal standards for distinguishing infiltrative marrow pathology from hematopoietic marrow at MRI. J Magn Reson Imaging 1997;7:394-8.
5. Vande Berg BC, Lecouvet FE, Galant C, Simoni P, Malghem J. Normal variants of the bone marrow at MR imaging of the spine. Semin Musculoskelet Radiol 2009;13:87-96.
6. Disler DG, McCauley TR, Ratner LM, Kesack CD, Cooper JA. In-phase and out-of-phase MR imaging of bone marrow: Prediction of neoplasia based on the detection of coexistent fat and water. AJR Am J Roentgenol 1997;169:1439-47.
7. Zampa V, Cosottini M, Michelassi C, Ortori S, Bruschini L, Bartolozzi C. Value of opposed-phase gradient-echo technique in distinguishing between benign and malignant vertebral lesions. Eur Radiol 2002;12:1811-8.
8. Padhani AR, Koh DM, Collins DJ. Whole-body diffusion-weighted MR imaging in cancer: Current status and research directions. Radiology 2011;261:700-18.
9. Baur A, Stäbler A, Brüning R, Bartl R, Krödel A, Reiser M, *et al*. Diffusion-weighted MR imaging of bone marrow: Differentiation of benign versus pathologic compression fractures. Radiology 1998;207:349-56.
10. Ryu KN, Jin W, Ko YT, Yoon Y, Oh JH, Park YK, *et al*. Bone bruises: MR characteristics and histological correlation in the young pig. Clin Imaging 2000;24:371-80.
11. Navas A, Kassarjian A. Bone marrow changes in stress injuries. Semin Musculoskelet Radiol 2011;15:183-97.
12. Krestan CR, Nemec U, Nemec S. Imaging of insufficiency fractures. Semin Musculoskelet Radiol 2011;15:198-207.
13. Fredericson M, Jennings F, Beaulieu C, Matheson GO. Stress fractures in athletes. Top Magn Reson Imaging 2006;17:309-25.
14. Major NM, Helms CA. Sacral stress fractures in long-distance runners. AJR Am J Roentgenol 2000;174:727-9.
15. Miletic D, Sestan B, Pusic M, Civcarić T, Tudor A, Roth S, *et al*. Unusual consecutive sacral stress fractures in a female distant runner: A case report. Eur J Phys Rehabil Med 2012;48:283-7.
16. Obembe OO, Gaskin CM, Taffoni MJ, Anderson MW. Little Leaguer's shoulder (proximal humeral epiphysiolysis): MRI findings in four boys. Pediatr Radiol 2007;37:885-9.
17. Eng J, Westcott J, Better N. Stress fracture of the first rib in a weightlifter. Clin Nucl Med 2008;33:371-3.
18. Nakaji N, Fujioka H, Tanaka J, Sugimoto K, Yoshiya S, Fujita K, *et al*. Stress fracture of the olecranon in an adult baseball player. Knee Surg Sports Traumatol Arthrosc 2006;14:390-3.
19. Guha AR, Marynissen H. Stress fracture of the hook of the hamate. Br J Sports Med 2002;36:224-5.
20. Mamanee P, Neira C, Martire JR, McFarland EG. Stress lesion of the proximal medial ulna in a throwing athlete. A case report. Am J Sports Med 2000;28:261-3.
21. Soubrier M, Dubost JJ, Boisgard S, Sauvezie B, Gaillard P, Michel JL, *et al*. Insufficiency fracture. A survey of 60 cases and review of the literature. Joint Bone Spine 2003;70:209-18.
22. Grasland A, Pouchot J, Mathieu A, Paycha F, Vinceneux P. Sacral insufficiency fractures: An easily overlooked cause of back pain in elderly women. Arch Intern Med 1996;156:668-74.
23. Yamamoto T, Bullough PG. Spontaneous osteonecrosis of the knee: The result of subchondral insufficiency fracture. J Bone Joint Surg Am 2000;82:858-66.
24. Mitchell DG, Rao VM, Dalinka MK, Spritzer CE, Alavi A, Steinberg ME, *et al*. Femoral head avascular necrosis: Correlation of MR imaging, radiographic staging, radionuclide imaging, and clinical findings. Radiology 1987;162:709-15.
25. Kattapuram TM, Kattapuram SV. Spontaneous osteonecrosis of the knee. Eur J Radiol 2008;67:42-8.
26. Blum A, Roch D, Loeuille D, Louis M, Batch T, Lecocq S, *et al*. Bone marrow edema: Definition, diagnostic value and prognostic value. J Radiol 2009;90:1789-811.
27. Poll LW, Weber P, Bohm HJ, Ghassem-Zadeh N, Chantelau EA. Sudeck's disease stage 1, or diabetic Charcot's foot stage 0? Case report and assessment of the diagnostic value of MRI. Diabetol Metab Syndr 2010;2:60.
28. Zhao J, Li X, Bolbos RI, Link TM, Majumdar S. Longitudinal assessment of bone marrow edema-like lesions and cartilage degeneration in osteoarthritis using 3 T MR T1rho quantification. Skeletal Radiol 2010;39:523-31.
29. Englund M, Guermazi A, Roemer FW, Yang M, Zhang Y, Nevitt MC, *et al*. Meniscal pathology on MRI increases the risk for both incident and enlarging subchondral bone marrow lesions of the knee: The MOST Study. Ann Rheum Dis 2010;69:1796-802.
30. Lo GH, Hunter DJ, Nevitt M, Lynch J, McAlindon TE; OAI Investigators Group. Strong association of MRI meniscal derangement and bone marrow lesions in knee osteoarthritis: data from the osteoarthritis initiative. Osteoarthritis Cartilage 2009;17:743-7.
31. Crema MD, Roemer FW, Zhu Y, Marra MD, Niu J, Zhang Y, *et al*. Subchondral cystlike lesions develop longitudinally in areas of bone marrow edema-like lesions in patients with or at risk for knee osteoarthritis: Detection with MR imaging--the MOST study. Radiology 2010;256:855-62.
32. Zanetti M, Bruder E, Romero J, Hodler J. Bone marrow edema pattern in osteoarthritic knees: correlation between MR imaging and histologic findings. Radiology 2000;215:835-40.
33. Yamamoto T, Kubo T, Hirasawa Y, Noguchi Y, Iwamoto Y, Sueishi K. A clinicopathologic study of transient osteoporosis of the hip. Skeletal Radiol 1999;28:621-7.
34. Vande Berg BE, Malghem JJ, Labaisse MA, Noel HM, Maldague BE. MR imaging of avascular necrosis and transient marrow edema of the femoral head. Radiographics 1993;13:501-20.
35. Conway WF, Totty WG, McEnery KW. CT and MR imaging of the hip. Radiology 1996;198:297-307.
36. Vande Berg BC, Lecouvet FE, Koutaissoff S, Simoni P, Malghem J. Bone marrow edema of the femoral head and transient osteoporosis of the hip. Eur J Radiol 2008;67:68-77.
37. Vande Berg BC, Malghem JJ, Lecouvet FE, Jamart J, Maldague BE. Idiopathic bone marrow edema lesions of the femoral head: predictive value of MR imaging findings. Radiology 1999;212:527-35.
38. Erly WK, Oh ES, Outwater EK. The utility of in-phase/opposed-phase imaging in differentiating malignancy from acute benign compression fractures of the spine. AJNR Am J Neuroradiol 2006;27:1183-8.
39. Eito K, Waka S, Naoko N, Makoto A, Atsuko H. Vertebral neoplastic compression fractures: Assessment by dual-phase chemical shift imaging. J Magn Reson Imaging 2004;20:1020-4.
40. Zajick DC Jr, Morrison WB, Schweitzer ME, Parellada JA, Carrino JA. Benign and malignant processes: Normal values and differentiation with chemical shift MR imaging in vertebral marrow. Radiology 2005;237:590-6.
41. Chan JH, Peh WC, Tsui EY, Chau LF, Cheung KK, Chan KB, *et al*.

Acute vertebral body compression fractures: Discrimination between benign and malignant causes using apparent diffusion coefficients. Br J Radiol 2002;75:207-14.

42. Herneth AM, Philipp MO, Naude J, Funovics M, Beichel RR, Bammer R, *et al*. Vertebral metastases: Assessment with apparent diffusion coefficient. Radiology 2002;225:889-94.
43. Byun WM, Shin SO, Chang Y, Lee SJ, Finsterbusch J, Frahm J. Diffusion-weighted MR imaging of metastatic disease of the spine: Assessment of response to therapy. AJNR Am J Neuroradiol 2002;23:906-12.
44. Yasumoto M, Nonomura Y, Yoshimura R, Haraguchi K, Ito S, Ohashi I, *et al*. MR detection of iliac bone marrow involvement by malignant lymphoma with various MR sequences including diffusion-weighted echo-planar imaging. Skeletal Radiol 2002;31:263-9.
45. Herneth AM, Friedrich K, Weidekamm C, Schibany N, Krestan C, Czerny C, *et al*. Diffusion weighted imaging of bone marrow pathologies. Eur J Radiol 2005;55:74-83.
46. Ozgen B, Oguz KK, Cila A. Diffusion MR imaging features of skull base osteomyelitis compared with skull base malignancy. AJNR Am J Neuroradiol 2011;32:179-84.
47. Abdel Razek A, Mossad A, Ghonim M. Role of diffusion-weighted MR imaging in assessing malignant versus benign skull-base lesions. Radiol Med 2011;116:125-32.
48. Pui MH, Mitha A, Rae WI, Corr P. Diffusion-weighted magnetic resonance imaging of spinal infection and malignancy. J Neuroimaging 2005;15:164-70.
49. Khoo MM, Tyler PA, Saifuddin A, Padhani AR. Diffusion-weighted imaging (DWI) in musculoskeletal MRI: A critical review. Skeletal Radiol 2011;40:665-81.
50. Wang CK, Li CW, Hsieh TJ, Chien SH, Liu GC, Tsai KB. Characterization of bone and soft-tissue tumors with *in vivo* 1H MR spectroscopy: Initial results. Radiology 2004;232:599-605.
51. Li X, Kuo D, Schafer AL, Porzig A, Link TM, Black D, *et al*. Quantification of vertebral bone marrow fat content using 3 Tesla MR spectroscopy: Reproducibility, vertebral variation, and applications in osteoporosis. J Magn Reson Imaging 2011;33:974-9.
52. Ledermann HP, Morrison WB, Schweitzer ME. MR image analysis of pedal osteomyelitis: Distribution, patterns of spread, and frequency of associated ulceration and septic arthritis. Radiology 2002;223:747-55.
53. Collins MS, Schaar MM, Wenger DE, Mandrekar JN. T1-weighted MRI characteristics of pedal osteomyelitis. AJR Am J Roentgenol 2005;185:386-93.
54. Ledermann HP, Morrison WB. Differential diagnosis of pedal osteomyelitis and diabetic neuroarthropathy: MR Imaging. Semin Musculoskelet Radiol 2005;9:272-83.
55. Toledano TR, Fatone EA, Weis A, Cotten A, Beltran J. MRI evaluation of bone marrow changes in the diabetic foot: A practical approach. Semin Musculoskelet Radiol 2011;15:257-68.
56. Donovan A, Schweitzer ME. Use of MR imaging in diagnosing diabetes-related pedal osteomyelitis. Radiographics 2010;30:723-36.
57. Roberts MC, Kressel HY, Fallon MD, Zlatkin MB, Dalinka MK. Paget disease: MR imaging findings. Radiology 1989;173:341-5.
58. Vande Berg BC, Malghem J, Lecouvet FE, Maldague B. Magnetic resonance appearance of uncomplicated Paget's disease of bone. Semin Musculoskelet Radiol 2001;5:69-77.
59. García AI, Milinkovic A, Tomás X, Rios J, Pérez I, Vidal-Sicart S, *et al*. MRI signal changes of the bone marrow in HIV-infected patients with lipodystrophy: Correlation with clinical parameters. Skeletal Radiol 2011;40:1295-1301.
60. Padhani AR. Diffusion magnetic resonance imaging in cancer patient management. Semin Radiat Oncol 2011;21:119-40.

Cite this article as: Grande FD, Farahani SJ, Carrino JA, Chhabra A. Bone marrow lesions: A systematic diagnostic approach. Indian J Radiol Imaging 2014;24:279-87.

Source of Support: Grants: Avneesh Chhabra acknowledges the support of research grants from Siemens AG and Integra Life Sciences as well as the support of a GE-AUR Fellowship. John A. Carrino (jcarrin2@jhmi.edu) acknowledges grant from Siemens Medical Systems. Filippo Del Grande (fdelgra1@jhmi.edu") acknowledges. Sahar J Farahani (sjalali2@jhmi.edu") has no grant to claim, **Conflict of Interest:** None declared.